2016 IEEE International Symposium on
Safety, Security, and Rescue Robotics (SSRR)
EPFL, Lausanne, Switzerland, October 23-27, 2016

Gait Design of a Snake Robot by Connecting Simple Shapes*

Tatsuya Takemori[1], Motoyasu Tanaka[2], Fumitoshi Matsuno[1]

Abstract— **This paper presents a method for expressing the target form of a snake robot by connecting simple shapes. Because the characteristics of each combined shapes are clear, we can intuitively design the target form and fit a snake robot to this form. In addition, we propose two novel gaits for the snake robot as a design example of the proposed method. The first gait is for pipe climbing to move over a flange on the pipe, while the other is the "Crawler-Gait" aimed at moving at high speed over uneven terrain. We demonstrate the effectiveness of each gait on a pipe, step, and set of stairs in a physical simulation.**

I. Introduction

Although snakes have a simple form without limbs, they can accomplish a variety of functions. For example, they use their bodies as legs when moving and as hands when grasping something. A snake robot, which is an engineered application of the mechanism of a snake, is expected to perform a wide variety of tasks. This property can be applied to disaster response. Because snake robots are suitable to enter narrow spaces and move over uneven ground, they can be used to explore the collapsed buildings. Since ground load is dispersed, secondary collapse is less likely to occur. In addition, by climbing pole-like objects, it is also possible to look around the environment from a high place.

Various gaits have been realized by determining the trajectory of the joint angle of the snake-like robot as a parameterized equation as given in [1]. However, if the desired form of a snake robot is too complex to express the joint angle with such a equation, it is difficult to find suitable joint angles by which it can be realized. In the method proposed in [2], [4], [5], the target form of a snake robot is expressed as a continuous curve and the body of the snake robot is approximately fitted to the curve. This method is particularly effective in realizing complex shapes. Methods for fitting a multi-link robot serially connected by a joint with two degrees of freedom to a target continuous curve are proposed [2], [3]. However, if each joint of the robot has only one degree of freedom, it is impossible to make all joints match on the curve. Hatton et al. [4] proposed *annealed chain fitting*, which can be applied to a snake robot whose joints only have a single degree of freedom. In this method, the approximate fitting of angles from the head to the tail of the robot is performed by minimizing an fitness function with respect to the error between the target curve and the robot's shape. However, the computational cost is high because the method involves solving a nonlinear equation. Thus, if the method were used for online control, it would be necessary to perform the calculations for the required shape in advance. In contrast, Yamada et al. [5] proposed a method for determining the target joint angles of the snake robot based on the curvature and torsion; the method achieves a good approximation in spite of the low computational cost.

Kamegawa et al. [6], [7] approximated a snake robot to a helical curve by applying Yamada's method, and realized climbing inside and outside a cylinder by lateral rolling. Furthermore, having created a smooth target curve by connecting the helix and *bending helical curve* [8], they implemented a robot that could propel along a curved pipe. Zhen proposed a *rolling hump* [9], where the curve is a superposition of a circular arc and a humped curve, and it is possible to negotiate obstacles locally by lifting up the body.

In [6]–[9], curvature and torsion are calculated from the target form represented as a continuous curve, and the target joint angles are calculated from the curvature and torsion of a continuous curve using Yamada's method [5]. However, if the target form is more complex, it is difficult to represent the target form analytically. Even if it could be represented analytically, there is another problem. According to [10], in the case where the target curve contains a part with zero curvature, its torsion would diverge to infinity in some cases. Then, it is impossible to calculate the target angle of the robot using the method given in [5].

In this paper, we propose a method for representing the target form of a snake robot by connecting simple shapes. The method enables us to intuitively design the target form because the characteristics of simple shapes are analytically clear. Furthermore, the curvature and torsion of simple shapes are already known. In addition, we propose two novel gaits for a snake robot designed using the proposed method. The first gait enables moving over a flange on a pipe. By this gait, the snake robot lifts up its body locally around the obstacle, retaining enough friction to prevent itself from dropping off the pipe. The other gait is the *Crawler-Gait*, which enables the robot to move at high speed over uneven ground. This gait can easily adapt to uneven ground because the body of the snake robot behaves like a large crawler belt. Simulations on a physical simulator demonstrate the effectiveness of each gait on a pipe, step, and set of stairs.

*This work was partially supported by the ImPACT Program of the Council for Science, Technology and Innovation (Cabinet Office Government of Japan).

[1]T. Takemori and F. Matsuno are with the Department of Mechanical Engineering and Science, Graduate School of Engineering, Kyoto University, Kyoto, 606-8501, Japan takemori.tatsuya.23a@st.kyoto-u.ac.jp, matsuno@me.kyoto-u.ac.jp

[2]M. Tanaka is with the Department of Mechanical and Intelligent Systems Engineering, The University of Electro-Communications, Tokyo 182-8585, Japan mtanaka@uec.ac.jp

978-1-5090-4349-1/16/$31.00 ©2016 IEEE

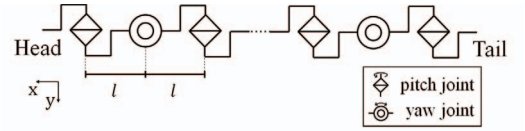

Fig. 1. Structure of a snake robot

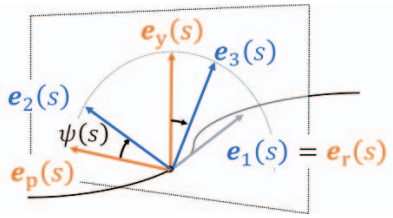

Fig. 2. Difference of Frenet–Serret frame and backbone curve frame

II. Shape Fitting Using Backbone Curve

We used a simulated snake robot model with several links serially connected by a pitch joint and a yaw joint as shown in Fig. 1. The lengths of all links are defined as l, while the angle of the i-th joint is defined as θ_i. The angle of each joint can be individually controlled.

We used Yamada's method [5], [10] to calculate the joint angles of the robot because of its low computational cost. This section follows Yamada's method [5], [10].

In Fig. 2, $\boldsymbol{e}_1(s), \boldsymbol{e}_2(s)$, and $\boldsymbol{e}_3(s)$ are unit vectors forming the orthonormal basis, called the Frenet–Serret frame. s is the variable of length along the curve. $\boldsymbol{e}_1(s)$ is a tangential vector to the curve at s, $\boldsymbol{e}_2(s)$ is a vector that indicates the direction of changing the curve at s, and $\boldsymbol{e}_3(s)$ is given by $\boldsymbol{e}_1(s) \times \boldsymbol{e}_2(s)$. This coordinate system is dependent on the shape of the curve. In contrast to the Frenet–Serret model, to model a snake robot, it is necessary to consider the joint direction. As shown in Fig. 2, a backbone curve reference set $\boldsymbol{e}_r(s)$, $\boldsymbol{e}_p(s)$, $\boldsymbol{e}_y(s)$ is defined on the curve by regarding the snake robot as a continuous curve. $\boldsymbol{e}_r(s)$ is equal to $\boldsymbol{e}_1(s)$. $\boldsymbol{e}_p(s)$ and $\boldsymbol{e}_y(s)$ are unit vectors oriented in the rotational direction around the pitch axis and yaw axis at s, respectively. These are defined as the basis vectors of the body coordinate system, which is determined by the orientation of each part of the robot.

As shown in Fig. 2, the twist angle of the Frenet–Serret frame and backbone curve reference set around $\boldsymbol{e}_1(s)$ is defined as $\psi(s)$, which can be expressed as

$$\kappa_p = -\kappa(s)\sin\psi(s), \tag{1}$$

$$\kappa_y = \kappa(s)\cos\psi(s), \tag{2}$$

$$\psi(s) = \int_0^s \tau(\hat{s})\mathrm{d}\hat{s} + \psi(0). \tag{3}$$

Here $\kappa(s)$ and $\tau(s)$ are the curvature and torsion in the Frenet–Serret formulas. $\kappa_p(s)$ and $\kappa_y(s)$ are the curvature around the pitch axis and yaw axis in the backbone curve reference set, respectively. $\psi(0)$ is the arbitrary integral constant corresponding to the initial angle. By changing $\psi(0)$, the entire body coordinate system rotates around the curve and a rolling motion is generated.

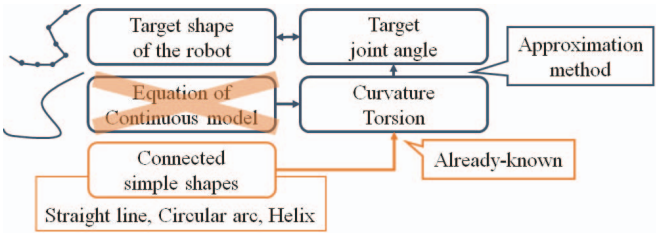

Fig. 3. Overview of the proposed method

The target angles of each joint are calculated as

$$\theta_i^d = \begin{cases} \int_{s_\mathrm{h}+(i-1)l}^{s_\mathrm{h}+(i+1)l} \kappa_p(s)\mathrm{d}s & (i:\mathrm{odd}) \\ \int_{s_\mathrm{h}+(i-1)l}^{s_\mathrm{h}+(i+1)l} \kappa_y(s)\mathrm{d}s & (i:\mathrm{even}) \end{cases}, \tag{4}$$

where s_h is the head position of the snake robot on a target continuous curve. The robot can move by *shift control* by changing s_h because the region corresponding to the body of the robot in the curve changes.

III. Backbone Curve Connecting Simple Shape

It is difficult to represent a complex target form of a snake robot analytically. There is also another problem: torsion would become extremely large if some part of the target form were straight. In this paper, we propose a method in which a target form is represented by connecting simple shapes the curvature and torsion of which are known. Using this method, calculation of the joint angles is easy because the curvature and torsion are known. Moreover, we can intuitively design the target form as a combination of simple shapes. We call a shape element connected in the method a *segment*, and describe how to configure the target form by connecting these segments.

A. Form configuration by connecting segments

An overview of our approach is shown in Fig. 3, while the approximation method is described in Section II. There is no problem with the approximation method for internal parts of segments because the curvature and torsion of each segment are already known. However, since the Frenet–Serret frame becomes discontinuous at the part where segments are connected, it is necessary to devise a representation at these connection-parts. Counting from the beginning, the j-th segment is referred to as *segment-j*($j \in \mathbb{Z}$). $s = s_j$ is the point of connection-part-j connecting segment-j and segment-$(j+1)$. The head position of the first segment is defined as s_0. Then, the length of segment-j l_j satisfy following relation:

$$s_j = s_{j-1} + l_j. \tag{5}$$

Segment-j and segments-$(j+1)$ must be in contact with each other at $s = s_j$. The state of connection-part-j is shown in Fig. 4. s_{j-} and s_{j+} are the points immediately before and after connection-part-j, respectively. They are determined as

$$s_{j-} = \lim_{\epsilon\to 0} s_j - \epsilon, \tag{6}$$

$$s_{j+} = \lim_{\epsilon\to 0} s_j + \epsilon, \tag{7}$$

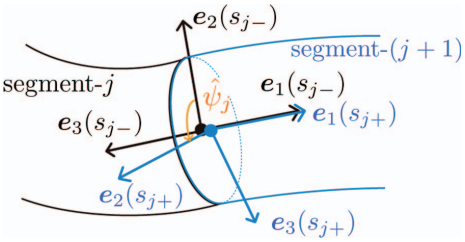

Fig. 4. Joint of segment

TABLE I
CHARACTERISTICS OF EACH TYPE OF SEGMENT

type	curvature κ_j	torsion τ_j	length l_j
helix	$a_j/(a_j^2+b_j^2)$	$b_j/(a_j^2+b_j^2)$	$\phi_i\sqrt{a_j^2+b_j^2}$
circular arc	$1/r_j$	0	$\phi_j r_j$
straight line	0	0	l_j

where $s = s_{j-}$ is the end of segment-j, and $s = s_{j+}$ is the beginning of segment-$(j+1)$. The Frenet–Serret frame, curvature, and torsion at $s = s_j$ are represented by those at $s = s_{j-}$.

Next, we consider the twisting at a connection-part. As shown in Fig. 4, the angle between $\boldsymbol{e}_2(s_{j-})$ and $\boldsymbol{e}_2(s_{j+})$ around $\boldsymbol{e}_1(s_{j-})$ is defined as $\hat{\psi}_j$. $\hat{\psi}_j$ is the twist angle, and is one of the design parameters. To consider this twist in the calculation of the approximation method, (3) must be replaced by

$$\psi(s) = \int_0^s \tau(\hat{s})\mathrm{d}\hat{s} + \psi(0) + \sum_j \hat{\psi}_j u(s - s_j), \quad (8)$$

where $u(s)$ is the following step function:

$$u(s) = \begin{cases} 0 & (s < 0) \\ 1 & (s \geq 0). \end{cases} \quad (9)$$

Therefore, if the curvature and torsion of each segment are known, the joint angles of the snake robot can be obtained by (1), (2), (4), and (8). To design a target form, we have to determine the shape of each segment and the twist angle $\hat{\psi}_j$.

B. Characteristics of simple shapes

We use a helix, circular arc, and straight line as the shapes for a segment because these are the simplest shapes whose curvature and torsion are constant. Note that any shape would be applicable if its curvature and torsion were clear. The characteristics of each segment are summarized in Table I. The helix (which refers to a normal helix in this paper) is a curve whose curvature and torsion have non-zero constant values. The radius a_j, slope b_j, and central angle ϕ_j define the shape of a helix. The helical pitch p_j, that is, the height of a coil, is given as

$$b_j = p_j/(2\pi). \quad (10)$$

α_j is the angle between the tangent of the helix and the plane perpendicular to the axis of the helix, and can be calculated as

$$\alpha_j = \arctan(b_j/a_j). \quad (11)$$

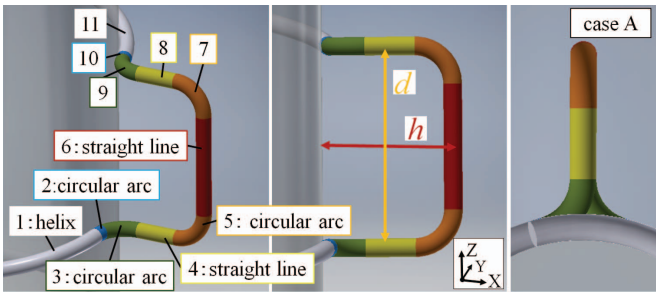

Fig. 5. Overview of the form in case A

$\boldsymbol{e}_2(s)$ is a unit vector directed to draw down a vertical segment on the axis of the helix from $\boldsymbol{c}(s)$. In a circular arc, curvature is constant and torsion is zero. The shape of the circular arc is defined by its radius r_j and central angle ϕ_j. In a straight line, the Frenet–Serret frame and torsion are not defined. In this paper, we newly define the frame and torsion for a straight line to handle straight segments in the same way as other segments. The frame inside the straight line is defined as being equal to the frame at $s = s_{j-}$ and torsion is zero.

IV. GAIT DESIGN

Using the representation method in Section III, we designed two novel gaits for the snake robot.

A. Moving over a flange on a pipe

Massimo et al. proposed the method for rolling on horizontal pipes with flanges [11]. However, it requires compliant elements in a snake robot structure and this method cannot be used for vertical pipe. In this paper, we proposed a novel gait that enables the snake robot to climb over flanges on pipes including vertical ones.

1) Design of a segment shape: It is possible for a snake robot to propel along a pipe through *helical rolling* [6], [7], [9]. In this gait, a *bridge part* is provided in the middle of a helix for passing over obstacles. The shape of the bridge part is determined by specifying the height and width of the bridge, as described later. Segment configuration of this form is divided into two cases, A and B, depending on the height of the bridge. The criteria for switching between the two cases are derived later.

First, we consider case A. Details of the segment configuration for case A, which is composed of 11 segments, are shown in Fig. 5. Both segment-1 and 11 are helixes with radius r_h and pitch p_h, and are long enough to cover the whole body of the robot. Pairs of segments, segment-2 and 10, segment-3 and 9, segment-4 and 8, and segment-5 and 7 have the same shape. Segment-6 is parallel to the helix axis, while segment-3, 4, 8, and 9 are on a plane perpendicular to the helix axis. Segment-5 and 7 are on the same or another plane parallel to the helix axis.

The radius of the circular arc are denoted by r_c. The height h of the bridge part is the distance between the cylinder and segment-6, and the width d is the distance between segment-4 and 8. Segment-4, 6, and 8 constitute the straight line

TABLE II

PARAMETERS OF SEGMENTS FOR THE MOTION OF CLIMBING OVER A FLANGE

index j	type	parameter	$\hat{\psi}_j$
1	helix	$(a_j, b_j) = (r_\mathrm{h}, p_\mathrm{h}/(2\pi))$	$-\pi/2$
2	circular arc	$(r_j, \phi_j) = (r_\mathrm{c}, \alpha_\mathrm{h})$	$-\pi/2$
3	circular arc	$(r_j, \phi_j) = (r_\mathrm{c}, \beta)$	0
4	straight line	$l_j = l_\mathrm{s}$	$-\pi/2$
5	circular arc	$(r_j, \phi_j) = (r_\mathrm{c}, \pi/2)$	0
6	straight line	$l_j = d - 2r_\mathrm{c}$	γ
7	circular arc	$(r_j, \phi_j) = (r_\mathrm{c}, \pi/2)$	0
8	straight line	$l_j = l_\mathrm{s}$	$\pi/2$
9	circular arc	$(r_j, \phi_j) = (r_\mathrm{c}, \beta)$	$\pi/2$
10	circular arc	$(r_j, \phi_j) = (r_\mathrm{c}, \alpha_\mathrm{h})$	$\pi/2$
11	helix	$(a_j, b_j) = (r_\mathrm{h}, p_\mathrm{h}/(2\pi))$	-

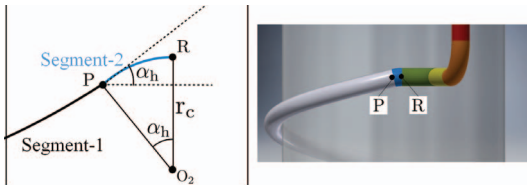

Fig. 6. Diagram of segment-2

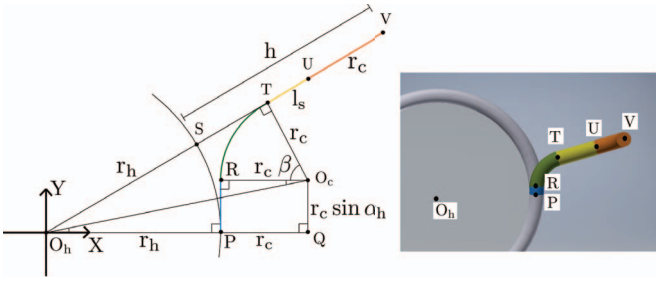

Fig. 7. Diagram of segment-1 to 5 in case A

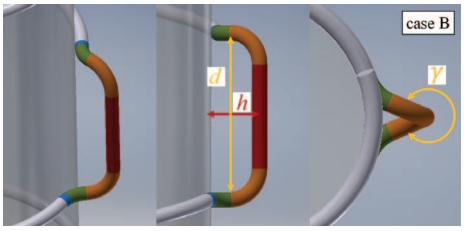

Fig. 8. Overview of the form in case B

with a length of zero or more, and satisfying the following relationship:

$$d \geq 2r_\mathrm{c}. \tag{12}$$

To configure the target form, the parameters of each segment are determined as given in Table II. The central angle of segment-2 and 10 α, central angle of segment-3 and 9 β, twist angle between segment-6 and 7 γ, and the length of the straight line comprising segment-4 and 8 l_s are derived from the geometric relationship. Segment-2 and 10 comprise a circular arc for changing the direction to be perpendicular to the axis of the helix by canceling the inclination of the helix. The diagram on the left of Fig. 6 shows the projection of segment-1 and a cylinder onto a plane containing segment-2. O_2 represents the center of the circular arc in segment-2. When the slope of the tangent of the helix is α_h, the central angle of segment-2 is determined as α_h.

The diagram on the left of Fig. 7 shows the projection of segment-1 to 5 onto a plane perpendicular to the helical axis. O_h is the intersection point of the plane and axes of the helix. Line segments PR and UV are projections of segment-2 and 5, respectively, while arc PS is the projection of segment-1 where r_h is the radius of the arc. O_c is the center of the arc of segment-3. O_hS, ST, TU, and UV are on the same straight line. From Fig. 7, β, l_s, and γ are determined by the following equation:

$$\begin{aligned}\beta &= \angle \mathrm{O_h O_c T} - \angle \mathrm{O_h O_c R} \\ &= \arccos\left(r_\mathrm{c}/\sqrt{(r_\mathrm{h}+r_\mathrm{c})^2 + (r_\mathrm{c}\sin\alpha_\mathrm{h})^2}\right) \\ &\quad - \arctan\left(r_\mathrm{c}\sin\alpha_\mathrm{h}/(r_\mathrm{h}+r_\mathrm{c})\right) \qquad (13) \\ l_\mathrm{s} &= h - \mathrm{ST} - \mathrm{UV} \\ &= h - \sqrt{(r_\mathrm{c}\sin\alpha_\mathrm{h})^2 + 2r_\mathrm{h}r_\mathrm{c} + r_\mathrm{h}^2} + r_\mathrm{h} - r_\mathrm{c} \qquad (14)\end{aligned}$$

$$\gamma = 0. \tag{15}$$

The value of h in case $l_\mathrm{s} = 0$ is the border of cases A and B. From (14), the border height h_b is determined as:

$$h_\mathrm{b} = \sqrt{(r_\mathrm{c}\sin\alpha_\mathrm{h})^2 + 2r_\mathrm{h}r_\mathrm{c} + r_\mathrm{h}^2} - r_\mathrm{h} + r_\mathrm{c}. \tag{16}$$

The case with $h > h_\mathrm{b}$ is case A.

The target form in case B ($h < h_\mathrm{b}$), is shown in Fig. 8. The length of segment-4 and 8 l_s is zero. β and γ are obtained from a different geometric relationship as in case A.

2) Combining shift control and rolling: As shown at the top of Fig. 9, when executing only shift control, the position of the bridge part relative to the flange would not be constant and the robot would collide with the flange. As shown at the bottom of Fig. 9, to keep the bridge part across the flange when passing over it, rolling motion should be carried out while executing shift control. The relationship between the shift length Δs and the amount of change of the bridge part is shown in Fig. 10. Then, Δs and the rotation angle $\Delta\psi$ must satisfy the following relation:

$$\Delta\psi \frac{d_\mathrm{robot}}{2}\cos\alpha_\mathrm{h} = -\Delta s \sin\alpha_\mathrm{h}, \tag{17}$$

where d_robot is the diameter of the trunk of the snake robot.

B. Crawler-Gait

We proposed the *Crawler-Gait*, which is capable of high-speed movement even while traversing rough terrain. This gait has higher adaptability to uneven ground because the body of the snake robot behaves like a large crawler belt similar to the *Loop-Gait* in [12], [13]. Further, because it does not require a special mechanism to connect the two ends of the robot, it is possible to apply this gait to a variety of snake-like robots. Because more than one part are grounded, the Crawler-Gait has greater stability and is

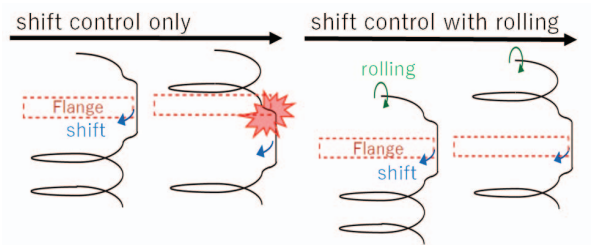

Fig. 9. Movement over a flange. Top: shift control only leads to the robot colliding with the flange. Bottom: Combined rolling with shift control avoids a collision

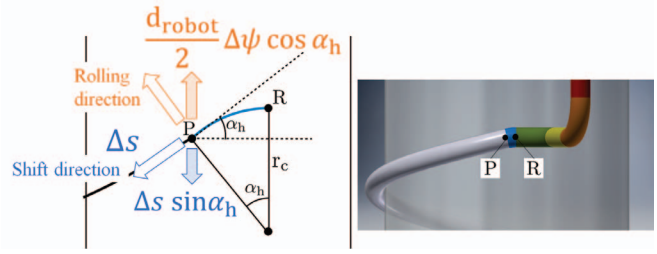

Fig. 10. Relationship between Δs and $\Delta\hat{\psi}_0$

suitable for movement across uneven terrain. In addition, the Crawler-Gait allows the robot to move faster than propulsion using the *Pedal-Gait* [14], while the width required for the motion is less than that for *Sidewinding* [15]. Segment configuration of the Crawler-Gait is shown in Fig. 11. This form is designed by connecting a unit consisting of six segments repeatedly. The straight line segments touch the ground whereas the circular arc segments are floating. By setting three values, namely, height h, width w and margin of the distance between the circular arcs d, the target form is determined as given in Table III. r_c is radius of circular arcs and α is torsion angle between circular arcs. These are obtained as follow:

$$r_c = \frac{\sqrt{h^2 + \left(\frac{w}{2}\right)^2}}{2} \quad (18)$$

$$\alpha = 2\arctan\frac{w}{2h}. \quad (19)$$

It is possible to propel in the x-axis direction in Fig. 11 with shift control. In addition, because the snake robot can move in the y-axis direction by rolling, it is capable of omni-directional movement.

TABLE III

PARAMETERS OF SEGMENTS FOR CRAWLER-GAIT

index $j(n \in \mathbb{Z})$	type	parameter	$\hat{\psi}_j$
$6n+1$	straight line	$l_j = 2r_c + d$	0
$6n+2$	circular arc	$(r_j, \phi_j) = (r_c, \pi)$	α
$6n+3$	circular arc	$(r_j, \phi_j) = (r_c, \pi)$	0
$6n+4$	straight line	$l_j = 2r_c + d$	0
$6n+5$	circular arc	$(r_j, \phi_j) = (r_c, \pi)$	$-\alpha$
$6n+6$	circular arc	$(r_j, \phi_j) = (r_c, \pi)$	0

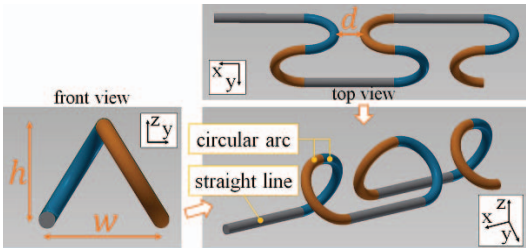

Fig. 11. Segment configuration of Crawler-Gait

V. SIMULATION

To verify the effectiveness of the two proposed gaits, we carried out simulations using the physical simulator COPPELIA ROBOTICS's V-REP [16]. The number of joints was 31, link length was 80 mm, diameter of the robot was 80 mm, weight per link was 0.25 kg, and maximum joint torque was 4.0 Nm. These specifications are based on them of the experimental snake robot under development witch uses KONDO B3M-SC-1170-A as actuators. The joints were controlled with P control executed in V-REP with the P gain set to 1.0. The coefficients of friction between the robot and the whole environment were 0.5.

A. Moving over a flange on a pipe

Two simulations were carried out trying to move over a flange on a vertical pipe. Operation of the robot was achieved by entering commands via a keyboard. The thickness of the flange was 50 mm, and the diameters of the pipe and flange were 100 mm and 200 mm, or 200 mm and 300 mm, respectively. In both cases, the robot successfully moved over the flange. The result of the simulation is shown in Fig. 12. The text at the bottom of the figure gives the input of the operator at each time. If snake robot has a sensor such as a camera on its head, it is possible to adapt shape of *bridge part* for moving over obstacles.

B. Crawler-Gait

1) Step climbing: With the Crawler-Gait, circular arc segments are expected to behave as a wheel and be able to climb a step. In the simulation, the snake robot was simply instructed to propel towards the step, without any information of shape of the obstacle and any special controls instructing it to climb. The results show that it was able to climb a step with a height of 200 mm with $h = 200$ mm, $w = 300$ mm and $d = 160$ mm.

2) Stair climbing: The robot needs to climb stairs if it moves in a house, building, or plant. From the results of the simulation, the robot was able to climb stairs where the height of an individual step was 150 mm, the length of a stair tread was 300 mm, and gait parameters were $h = 150$ mm, $w = 300$ mm and $d = 160$ mm. Simulation result of this case is shown in Fig. 13. The parts in contact with the stairs ware pressed against the wall by the propulsion of the rear part of the robot, resulting in sufficient upward force. Because the robot was controlled based on P control and had maximum torque, it had compliances and adapted to the

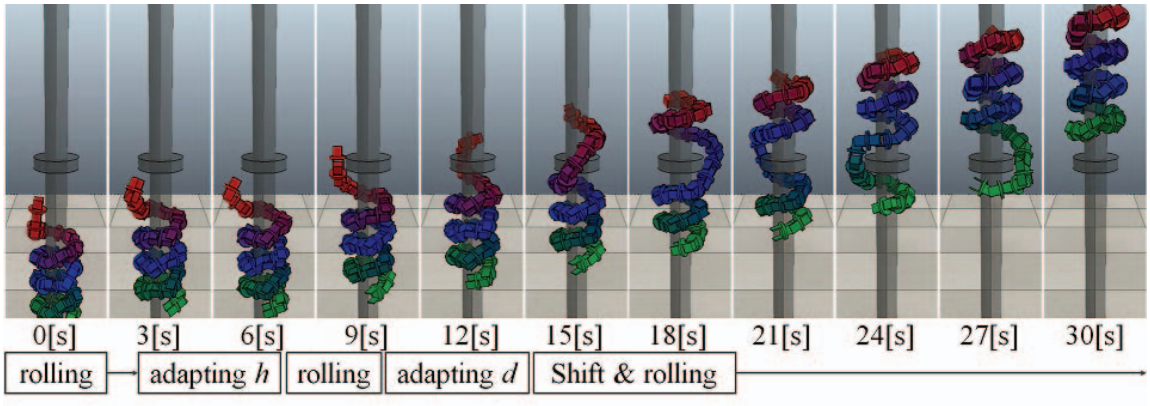

Fig. 12. Simulation result for moving over a flange on a 100 mm pipe

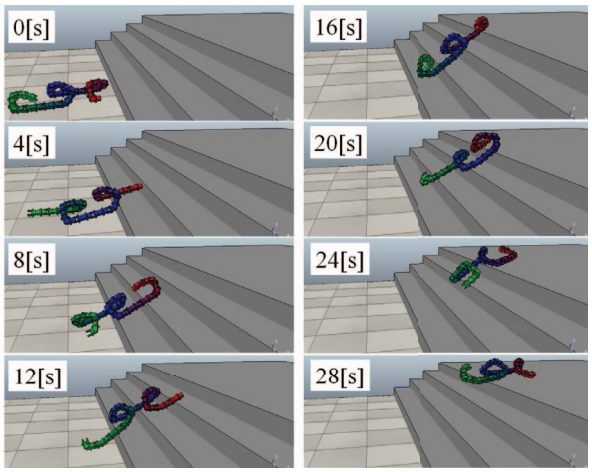

Fig. 13. Simulation result for climbing stairs

environment as a whole. These functions make it possible to move across uneven terrain while keeping a low center of gravity.

VI. Conclusion

In this study, we proposed a method for representing the target form of a snake robot by connecting simple shapes. This method allows complicated forms to be realized by approximating the snake robot to the target form expressed by this method. In addition, we proposed two novel gaits for a snake robot using the proposed method. The first gait allows a snake-robot to move on pipes with flanges. The robot was able to move over the flange in the physical simulation. The other gait is the Crawler-Gait aimed at moving at high speed, even over uneven terrain. According to the results of the physical simulation, the robot was able to climb a single step and a set of stairs with unknown size, without any special control based on shape of obstacls. Future works include the implementation of an experimental snake robot and experimental verification of the proposed gaits.

References

[1] M. Tesch, K. Lipkin, I. Brown, R. Hatton, A. Peck, J. Rembisz, and H. Choset, "Parameterized and Scripted Gaits for Modular Snake Robots," *Advanced Robotics*, vol. 23, no. 9, pp. 1131–1158, 2009.

[2] S. Andersson , "Discretization of a Continuous Curve," *IEEE Trans. on Robotics*, vol. 24, no. 2, pp. 456–461, 2008.

[3] P. Liljebck, K. Y. Pettersen, . Stavdahl and J.T. Gravdahl, "A 3D Motion Planning Framework for Snake Robots," *Proc. IEEE/RSJ Int. Conf. on Intelligent Robots and Systems* 2014, ,pp. 1100-1107.

[4] R.L. Hatton and H. Choset, "Generating gaits for snake robots: annealed chain fitting and keyframe wave extraction," *Auton. Robot*, vol. 28, no. 3, pp. 271–281, 2010.

[5] H. Yamada and S. Hirose, "Study of Active Cord Mechanism - Approximations to Continuous Curves of a Multi-joint Body-," *J. of the Robotics Society of Japan*, vol.26, no.1, pp.110–120, 2008. (Japanese)

[6] T. Kamegawa, T. Harada, and A. Gofuku, "Realization of cylinder climbing locomotion with helical form by a snake robot with passive wheels," *Proc. IEEE Int. Conf. on Robotics and Automation*, 2009, pp. 3067–3072.

[7] T. Baba, Y. Kameyama, T. Kamegawa, and A. Gofuku, "A snake robot propelling inside of a pipe with helical rolling motion," *Proc. SICE Annual Conference*, 2010, pp. 2319–2325.

[8] T. Kamegawa, T. Baba, and A. Gofuku, "V-shift control for snake robot moving the inside of a pipe with helical rolling motion," *Proc. IEEE Int. Symp. on Safety, Security, and Rescue Robotics*, 2011, pp. 1–6.

[9] W. Zhen, C. Gong, and H. Choset, "Modeling Rolling Gaits of A Snake Robot," *Proc. IEEE Int. Conf. on Robotics and Automation*, 2015, pp. 3741–3746.

[10] H. Yamada and S. Hirose, "Study on the 3d shape of active cord mechanism," *Proc. IEEE Int. Conf. on Robotics and Automation*, 2006, pp. 2890–2895.

[11] M. Vespignani, K. Melo, M. Mutlu, and A. J. Ijspeert "Compliant snake robot locomotion on horizontal pipes," *Proc. IEEE Int. Symp. Safety, Security Rescue Robot.*, 2015.

[12] M. Yim, D.G. Duff, and K.D. Roufas , "PlayBot: a modular reconfigurable robot," *Proc. IEEE Int. Conf. on Robotics and Automation*, 2000, pp. 514–520.

[13] T. Ohashi, H. Yamada, and S. Hirose, "Loop forming snake-like robot ACM-R7 and its serpenoid oval control," *Proc. IEEE/RSJ Int. Conf. on Intelligent Robots and Systems*, 2010, pp. 413–418.

[14] H. Ohno and S. Hirose, "Design of slim slime robot and its gait of locomotion," *Proc. IEEE/RSJ Int. Conf. on Intelligent Robots and Systems*, 2001, pp. 707–715.

[15] J.W. Burdick, J. Radford, and G.S. Chirikjian, "A "Sidewinding" Locomotion Gait for Hyper-Redundant Robots," *Advanced Robotics*, vol. 9, no. 3, pp. 195–216, 1995.

[16] COPPELIA ROBOTICS, "V-REP," http://www.coppeliarobotics.com/